UCRL-16840

University of California

Ernest O. Lawrence Radiation Laboratory

SPIN-LATTICE AND SPIN-SPIN RELAXATION TIMES FOR VO_2^+ IN AQUEOUS SOLUTION

TWO-WEEK LOAN COPY

This is a Library Circulating Copy which may be borrowed for two weeks. For a personal retention copy, call Tech. Info. Division, Ext. 5545

DISCLAIMER

This document was prepared as an account of work sponsored by the United States Government. While this document is believed to contain correct information, neither the United States Government nor any agency thereof, nor the Regents of the University of California, nor any of their employees, makes any warranty, express or implied, or assumes any legal responsibility for the accuracy, completeness, or usefulness of any information, apparatus, product, or process disclosed, or represents that its use would not infringe privately owned rights. Reference herein to any specific commercial product, process, or service by its trade name, trademark, manufacturer, or otherwise, does not necessarily constitute or imply its endorsement, recommendation, or favoring by the United States Government or any agency thereof, or the Regents of the University of California. The views and opinions of authors expressed herein do not necessarily state or reflect those of the United States Government or any agency thereof or the Regents of the University of California.

Summer Symposium on ESR Spectroscopy
American Chem. Soc., East Lansing,
Michigan.
August, 1966.

UCRL-16840

UNIVERSITY OF CALIFORNIA

Lawrence Radiation Laboratory
Berkeley, California

AEC Contract W-7405-eng-48

SPIN-LATTICE AND SPIN-SPIN RELAXATION TIMES FOR VO^{+2} IN AQUEOUS SOLUTION

Douglas C. McCain and Rollie J. Myers

April, 1966

Spin-Lattice and Spin-Spin Relaxation Times for VO^{+2} in Aqueous Solution

Douglas C. McCain and Rollie J. Myers

Inorganic Materials Research Division,
Lawrence Radiation Laboratory and
Department of Chemistry, University of California,
Berkeley, California

Abstract

A dynamic nuclear polarization spectrometer operating near 3,000 mc is described. This was used for the measurement of the relative electronic spin-lattice relaxation times for the eight hyperfine transitions of VO^{+2} in aqueous solution. The electronic spin-spin relaxation times for these eight hyperfine transitions were also measured. Comparison of both results is made with the theory developed by Kivelson, and, on the whole, excellent agreement is found.

INTRODUCTION

It is a relatively simple matter to determine the spin-spin relaxation times T_2 for transition metal ions in solution, and in most cases these fall in the range of 10^{-7} to 10^{-10} sec. The spin-lattice relaxation times T_1 of these ions is much more difficult to measure and little experimental work has been done on T_1. However, these T_1 values are important both for the interpretation of the NMR data of protons and O^{17} in aqueous solutions of these ions and for an understanding of the magnetic properties of these ions in solution. We have developed a dynamic nuclear polarization spectrometer which allows us to measure the electronic T_1 for many transition metal ions in aqueous solution. This spectrometer determines the nuclear polarization of the protons in water after conditions of relative saturation of the electron spins of the transition metal ions. This spectrometer is capable of determining T_1 values as short as 10^{-10} sec. even if T_2 is also that small.

This paper describes our apparatus and applies it to VO^{+2} in aqueous solution. The relative T_1 values have been measured for the eight hyperfine components of this ion and comparison is made to the theory of electron spin relaxation developed by Kivelson.[1]

EXPERIMENTAL

I. Dynamic Nuclear Polarization Spectrometer

In our dynamic nuclear polarization spectrometer, the high power S-band microwave energy necessary for saturation is supplied by a Raytheon QK625 backward wave oscillator. This tube can supply variable

amounts of power from 50 to about 250 watts at frequencies between 2500 and 3300 mc. Power supplies used to operate the tube must be very well regulated to keep the output stable because both frequency and power level are strong functions of input voltages. Microwave power as shown in Figure 1 travels through an isolator which prevents damage to the BWO from the large reflected power encountered during tune-up. An E-H tuner located after the isolator optimizes energy transfer to the cavity.

In order to calculate specific enhancements, the power incident on the cavity must be known accurately. Some of the power traveling toward the cavity is sampled by a 10 db. directional coupler from which it is sent through an FXR 0 to 50 db. attenuator (model S164A), into a Narda model 534 bolometer holder containing a Narda N605 bolometer. A Hewlett-Packard 430CR microwave power meter indicates the power reaching the bolometer. During the study of VO^{+2} ions, uncertainties in power measurement are believed to have been a major source of inaccuracy, resulting in a scatter of about ± 3% in the measured specific enhancements.

Another directional coupler with an attenuator, crystal detector and crystal current meter indicates the power reflected from the cavity. During tune-ups this signal is used to set the microwave frequency exactly on cavity resonance.

The cavity itself is a special, parabolic design, which was chosen after considerable experimentation with alternate designs. It is derived from a rectangular TE_{011} mode cavity with the narrow rectangular wall replaced by a parabola. Since the perturbation is in a modeless dimension, little change in resonant frequency of this mode is expected, and the only change in RF magnetic field distribution will be an increase

in field intensity at the narrow (sample) end of the cavity. The cavity is constructed of 0.01 inch silver sheet, soft soldered at all joints. Included is a "T" shaped quartz sample tube. A Q of about 5000 has been observed with the sample tube empty. With the 0.01M salt solutions normally used, Q is about 3000 with nearly critical coupling at 3110 mc.

The solutions are flowed through the cavity in order to limit temperature rise and to optimize both NMR sensitivity and cavity geometry. Sample solution is flowed into both ends of the 5 mm. ID. quartz sample tube and out at the center through the 3 mm. tube containing the NMR coil. The optimum flow rate for .01M VO^{+2} was 0.9 ℓ/min. At this flow rate the power used for saturation (normally 70 to 100 watts) will cause a temperature rise of less than 1.5°C for the solution inside the cavity. The sample is continuously recycled by pumping with an immersible "Teel" pump (model 1P597). Just before entering the cavity the sample passes through a coiled stainless steel heat exchanger which is immersed in a water bath.

The object of this design is to leave the sample in the microwave magnetic field for a time long compared to the nuclear spin-lattice relaxation time T_1 (nuclear), then to get it out of the cavity and into the NMR coil in a time short compared to T_1 (nuclear). This is because polarization both builds up and decays exponentially with the time constant T_1 (nuclear). As a measure of the success in achieving this, the observed polarization in the apparatus described is about one-half that which would be obtained in the same cavity if the sample were not flowing. Nuclear spin-lattice relaxation times in water are inversely proportional to the concentration of paramagnetic ions, therefore the

optimum flow rate is proportional to paramagnetic ion concentration.

The NMR used is a conventional, transistorized,[2] marginal oscillator. Magnetic field modulation and phase detection are used and the signal is displayed on a recorder. The NMR frequency is also used to measure the static magnetic field which is generated by a Varian 6 inch electromagnet.

In a typical experiment, the DC magnetic field is swept back and forth over a very small range covering the NMR line. NMR signals are recorded with microwave power off for several sweeps, then with power on, then off, then on, etc. During the power-on periods, the microwave frequency is kept exactly on the cavity resonance, and power input is noted.

The average signal intensity (height from NMR derivative peak to peak) is found and a specific enhancement E_{100} computed.

$$E_{100} = \left(1 - \frac{\text{ave. signal with power on}}{\text{ave. signal with power off}}\right) \frac{100}{\text{power input in watts}}$$

E_{100} is the enhancement normalized to that which would be observed at 100 watts output. From a number of experiments it has been concluded, in agreement with expectations for short T_1 (electronic), that at any given field, E_{100} is independent of the actual power input used. At very high powers (higher than are normally used, say 150 watts and up) a slight "enhancement" which is independent of DC magnetic field can be observed. This is probably due to heating of the water sample and subsequent change in NMR level.

Specific enhancements are measured at a number of fields chosen to coincide with line centers or simply regularly spaced fields used for

research purposes. Enhancements are then plotted as a function of field to give an enhancement spectrum.

The quantity E_{100} is dependent upon flow rate, cavity Q and a number of experimental variables. Within a run these variables are constant and with certain assumptions precise relative values for T_1 (electronic) can be calculated from E_{100} values. The precision of these determinations is primarily limited by our ± 3% uncertainty in the determination of power input.

II. Low Power S-band ESR Spectrometer

The S-band electron spin resonance (ESR) spectrometer used for the measurement of the electronic T_2 at 3,000 mc. is of fairly conventional design. A Hewlett-Packard 8616 A signal generator produces up to 50 mw. of power, which passes through an isolator into a magic-tee type reflection spectrometer. Modulation, amplification, and phase detection are accomplished by a Varian V4560 100 kc. field modulation and control unit.

The one unusual feature of this spectrometer is its cavity which is made of a block of fused quartz 2 13/16" x 1 5/16" x 3/8" with a 3/16" hole drilled through the exact center of the 2 13/16" x 3/8" faces. The block is coated with silver on five sides to a thickness of 2×10^{-4} inch. This was done by rotating it in a vacuum over a pot of boiling silver. Several other methods of coating which were tried gave unsatisfactory results. During the process, one face, 3/8" x 1 5/16" was masked off, as was the inside of the 3/16" hole through the block. The coated block was soft soldered to a sheet of 0.01 inch silver sheet with a 3/8" coupling hole, the uncoated face butting against the sheet and centered on

the coupling hole. The 0.01 inch sheet was soldered, with the coupling hole centered, to the open end of an S-band copper waveguide. The whole cavity was then coated with epoxy glue for rigidity and to preserve the silver coating. Modulation coils, $1\frac{1}{2}$" in diameter, were attached to the broad faces of the cavity.

The cavity resonant frequency is 3120 mc. and the unloaded Q is about 4500. The observed sensitivity of this spectrometer for VO^{+2} in aqueous solution is just about equal to that of the Varian X-band, 100 kc. modulated, V4500 spectrometer. One normally would expect that a 3000 mc. spectrometer should be less sensitive than one using 9000 mc. The difference is made up by the possible use of a larger sample due to the fact that water solutions are less lossy at the lower frequency and by the cavity design. For convenient temperature control the sample is pumped through a heat exchanger coil in a water bath, and continuously recycled.

III. Samples

$VOSO_4$ solutions were made by dissolving a weighed amount of $VOSO_4 \cdot 5H_2O$ in water. $VO(ClO_4)_2$ solutions were made by adding the proper amount of $Ba(ClO_4)_2$ to a $VOSO_4$ solution and filtering out the $BaSO_4$ precipitate. These solutions gave negative tests for the presence of Ba^{+2}, SO_4^{-2}, and Cl^-. To slow the air oxidation of VO^{+2}, all solutions were adjusted to pH 3 with $HClO_4$.

Samples were not degassed. Experiments with solutions saturated in O_2 indicate the broadening at 30° due to oxygen from dissolved air is less than 0.1 gauss. In sulfate solutions an excess line width is

seen which is linear in sulfate concentration. It contributes 0.34 gauss in 0.01M $VOSO_4$ at 30°C. This is presumed to arise because of ion pairing.[3]

A number of studies at different concentrations of VO^{+2} in the dynamic polarization spectrometer, show that within wide limits, its concentration is not an important variable. In the ESR spectrometer, too, it is found that linewidth of aqueous $VO(ClO_4)_2$ solutions is almost independent of concentration up to 0.1M. The self broadening reported[1] in vanadyl acetylacetonate is not found here presumably because of the charges on the VO^{+2} ions. If one were to compare the enhancement due to VO^{+2} with that of some other ion in order to find relative relaxation times, concentrations would have to be known to a greater accuracy.

Temperature is, however, a very important variable, and one that is difficult to control. Since the temperature varies through the cavity, an uncertainty of at least one degree must be expected. Temperature was monitored by a mercury thermometer immersed in the solution at the pump. This temperature, which might represent an average temperature of the system, varied between 28° and 30°, although attempts were made to keep it at 29°. An estimated 1° rise in temperature in the cavity brings the sample to a nominal 30°. In any case, it is not likely to be over 31° or under 28°. A change of 1° causes about a one percent change in linewith at these temperatures.

THEORY OF DYNAMIC NUCLEAR POLARIZATION

Dynamic nuclear polarization has been extensively discussed,[4] but we shall review a small part of this theory. In a system with many equivalent electron spins in a solvent containing equivalent nuclear spins

such as protons in water, if the spin systems are coupled then Abragam has shown that

$$< I_z > = I_o - \sigma/\rho \, [< S_z > - S_o] .$$

For a single paramagnetic species with $S = 1/2$ and with only dipole-dipole coupling with the protons in the solvent $\sigma/\rho \leq 1/2$. When an oscillating magnetic field $H_1 \cos \omega t$ is applied at the resonance frequency of the electron spins then

$$< S_z > = \frac{S_o}{1 + \gamma_e^2 H_1^2 T_{1e} T_{2e}} .$$

If the electron spin system is fully saturated

$$\gamma_e^2 H_1^2 T_{1e} T_{2e} \gg 1$$

and the nuclei are polarized so that

$$\frac{< I_z >}{I_o} = 1 + \sigma/\rho \, \frac{S_o}{I_o} .$$

For a system of protons and one paramagnetic species with $g = 2$

$\frac{S_o}{I_o} = -657$ and $\frac{< I_z >}{I_o} \approx -330$ when $\sigma/\rho \approx 1/2$.

In our apparatus, power is limited and only partial saturation is obtained. Under these conditions

$$\gamma_e^2 H_1^2 T_{1e} T_{2e} \ll 1$$

and

$$[< S_z > -S_o] = -S_o \gamma_e^2 H_1^2 T_{1e} T_{2e}$$

at the center of the resonance transition, or more generally for an excitation at a frequency ω not on the exact resonant frequency ω_e

$$< S_z > -S_o = \frac{-S_o \gamma_e^2 H_1^2 T_{1e} T_{2e}}{1 + (\omega - \omega_e)^2 T_{2e}^2}$$

Absolute values of H_1^2 are difficult to measure, and this is not attempted in the present experiment but since in our experiments $H_1^2 \alpha$ incident power

$$[< S_z > -S_o] \alpha \frac{S_o P_{in} T_{1e} T_{2e}}{1 + (\omega - \omega_e)^2 T_{2e}^2} .$$

We now define the enhancement, E, which is an experimentally observable quantity as

$$E = 1 - \frac{< I_z >}{I_o} = \frac{\sigma[< S_z > -S_o]}{\rho I_o} .$$

Since we operate at a fixed microwave frequency ω and S_o are constants but I_o is proportional to the static magnetic field H. In this case, we have for a single kind of electron spin

$$E_H \quad \alpha \quad \frac{\sigma P_{in} T_{1e} T_{2e}}{\rho H[1 + (\omega - \omega_e)^2 T_{2e}^2]} .$$

The preceding equation must be modified for VO^{+2} which has eight fairly well resolved hyperfine transitions. First, it must be summed over the eight m values for the nuclear spin of V^{51}. In this case ρ must be replaced by

$$\rho = \Sigma \rho_m$$

where from Abragam[4b]

$$\rho_m \propto 7 + \frac{3}{1 + \omega_{em}^2 \tau_c^2} .$$

The values of σ_m are given by

$$\sigma_m \propto \frac{1}{1 + \omega_{em}^2 \tau_c^2} .$$

So that to correct for overlapping absorptions

$$E_H \propto \frac{P_{in}}{\rho H} \sum_m \frac{\sigma_m T_{1em} T_{2em}}{1 + (\omega - \omega_{em})^2 T_{2em}^2} .$$

A further complication arises because there are terms in the spin relaxation which are not diagonal in m. They give a cross-relaxation so that $< S_z >_{m'} - S_{om'}$ is not zero even if it does not overlap with the transition m under conditions of partial saturation. Kivelson[1] gives the T_1 terms which are off-diagonal in m and contribute to cross-relaxation of the type

$$< S_z >_{m'} - S_{om'} = \delta_{m'm} [< S_z >_m - S_{om}] .$$

The values of $\delta_{m'm}$ drop off rapidly as m and m′ differ by more than unity. This effect can be included in our equation for E_H by defining σ_m as

$$\sigma_m = \sum_{m'} \sigma_{m'} \delta_{m'm}$$

where $\delta_{m'm} = 1$ for $m' = m$.

E.S.R. SPECTRA OF $VO(H_2O)_5^{+2}$

Vanadyl ion may be described by a spin Hamiltonian of the form:

$\mathcal{H} = \beta \bar{S} \cdot g \cdot \bar{H} + \bar{I} \cdot A \cdot \bar{S}$ where g and A are tensors.

In solution anisotropies average out. To second order, the observed transitions with $\Delta M = \pm 1$ and $\Delta m = 0$ at an excitation frequency ω are

$$\hbar \omega = g\beta H + a m + 1/2\, a^2 \left[\frac{I(I+1) - m^2}{g\beta H}\right]$$

$$a = 1/3\,(Ax + Ay + Az)$$

$$g = 1/3\,(gx + gy + gz)$$

At X-band the eight hyperfine transitions are observed at just the fields predicted but at S-band small third order corrections are necessary. Interest, however, attaches to the fact that the lines are all of different widths. In Figure 3 all eight lines have the same integrated intensity but different widths give a complex, unsymmetrical pattern.

Rodgers and Pake[5] studied this line width variation utilizing a theoretical treatment by Kivelson.[6] The more recent paper[1] considers more terms and has given good agreement for vanadyl acetylacetonate in liquid toluene. In order to make quantitative use of this theory we need values for the anisotropic elements of the Hamiltonian.

$VO(H_2O)_5^{+2}$ has C_{4v} symmetry and an axial spin Hamiltonian containing $A_{||}$, $A_{\perp}$, $g_{||}$ and $g_{\perp}$. Following the techniques developed by B. Spencer[7] we have examined the X-band spectrum of 0.1M $VOSO_4$ in 5.26M $HClO_4$ as a eutectic at 100°K. This glass gave an easily assigned 16 line spectrum and the resulting anisotropic constants are given in Table I. These values for g and $a/g\beta$ are in good agreement with the spectrum in aqueous solution. At S-band we find $\frac{a}{g\beta} = 118$ gauss and $g = 1.962$.

Wilson and Kivelson[1] show that T_{1e} and T_{2e} can be fit by a power series in m which we shall write as:

$$1/T_{1e} = \alpha_1' + \alpha_1 + \beta_1 m + \gamma_1 m^2 + \delta_1 m^3$$

$$1/T_{2e} = \alpha_2' + \alpha_2 + \beta_2 m + \gamma_2 m^2 + \delta_2 m^3$$

where α' is a relaxation due to any mechanism not considered in the theory. Theoretical values for α, β, γ and δ can be derived from the contributions given in Tables III and IV of reference 1.

SPIN-SPIN RELAXATION TIMES

Line widths of the eight hyperfine components were measured by two methods. The separation of the positive and negative peaks in the first derivative spectrum can be directly measured. One can also measure the relative height of the signal between the positive and negative peaks. One obtains from this the relative line widths by using the relation, strictly true only for identical line shape functions, that the square of line width is proportional to first derivative line height. We find these two methods are consistent within our experimental error.

Relative line widths from direct measurement agree with those derived from line heights although line height measurements are both easier and more precise, and we obtained a precision of ± 1%. For this work we directly measured the narrowest line, m = -3/2, which is the third line up from low field, and then from line heights calculated the other line widths. This same method has been used by other authors.[1,5]

Table II compares measured line widths with those calculated from an empirical fit to the power series equation. It can be seen that the four parameters do fit eight linewidths acceptably. Scatter due to experimental error shows an average deviation of .05 gauss at S-band and .04 gauss at X-band.

With the assumption of Lorentzian line shape Table III compares experimental linewidth parameters with those calculated from Kivelson's[1] rather complicated equations. To perform this calculation, one needs to know b, a, and Δg, all of which are given in Table I. One must also estimate the rotational correlation time τ_c. In Kivelson's model τ_c is the tumbling time for the $VO(H_2O)_5^{+2}$ complex. Since we neither know the effective radius of this complex nor the microscopic viscosity of water only approximate values of τ_c can be obtained from Debye's equation. If one uses a radius of 3.3A and macroscopic viscosity then $\tau_c \sim 3 \times 10^{-11}$ sec. Values near 3×10^{-11} sec. are commonly used in similar studies on other aqueous solutions. An examination of Table III will show that no one value of τ_c can fit all the data exactly, but that 3×10^{-11} sec. is a reasonable compromise. Smaller values give poorer fit to γ_2 and larger values do not fit β_2. γ_2 and δ_2 are fit rather well, considering the model.

Hydrated ions might be expected to deviate more from the theory than the vanadyl acetylacetonate used by Kivelson[1] because of the more intimate solvent-ion interactions.

Note that the β_2 predicted at S-band is considerably larger than the measured value, and that α_2', which is the difference between predicted and observed values of α_2, is about twice as large at S-band as it is at X-band. No reasonable variation of anisotropic constants will close the gap between α_2' at S-band and at X-band since the major difference predicted by the theory depends only on $1/1 + \omega^2\tau_c^2$. The difference could perhaps be made up by the terms in $(\frac{a}{\omega})^2$ which Kivelson[1] says he discarded in his calculations. They would be much more important at S-band than they are at X-band.

The data given are for $VOSO_4$. Solutions of either $VOSO_4$ or $VO(ClO_4)_2$ of up to .03M have identical values of β_2, γ_2 and δ_2. α_2 is a function of concentration in $VOSO_4$ and is increased by .34 gauss at .01M. α_2 for any $VO(ClO_4)_2$ solution below .03M is independent of concentration and is the same as the extrapolated zero concentration $VOSO_4$ value. Above .05M parameters of both $VOSO_4$ and $VO(ClO_4)_2$ deviate from their low concentration values. For example, in .1M $VO(ClO_4)_2$, α_2 = 13.00 gauss at X-band.

Some work was done on $VOSO_4$ solutions at other temperatures. These followed the temperature dependence expected from the macroscopic viscosity with α_2' having almost no temperature dependence. This indicates little spin-rotation contribution.[8] More extensive work[9] has also been done on $VO(ClO_4)_2$ solutions over a wide temperature range.

SPIN-LATTICE RELAXATION TIMES

Enhancements, E_{100}, were measured at a number of fields. Most of these fields did not exactly coincide with the center of a hyperfine absorption line. In Figure 5 a plot of normalized, measured enhancements is superimposed on Lorentzian line shape functions which were calculated to have widths equal to those observed in the low power ESR. The absorption line shown is centered on the m = 1/2 hyperfine transition. A slight upturn at both edges of the figure is due to overlap contributions from the m = -1/2 and m = 3/2 transitions. The excellent fit between experimental points and the theoretical curve shows that we are justified in assuming a Lorentzian line shape when we analyze our data.

In order to use more of the data, points measured at fields which were near the line centers were corrected to a line center value. This correction was made by the assumption of a Lorentzian line shape with a T_{2e} derived from the line width observed in the low power ESR spectrum. Corrected values calculated in this way agreed well with measured line center E_{100} values. Both kinds of points were averaged together to give line center E_{100} values for each run. Average line center E_{100} values varied a bit from one run to the next. For example, in .01M $VO(ClO_4)_2$, E_{100} for m = 1/2 ranged between the limits of .3029 and .3477. The causes of this experimental scatter are not fully understood, but it was noted that enhancements were more consistent than this within the data for any single run. So to eliminate errors from these spurious effects we normalize each day's data, assigning that same run m = 1/2 enhancement

an arbitrary value of 1.0. Normalized data from all days are then averaged together. The m = 1/2 line was chosen as a standard because it is in the center of the spectrum, lending convenience, and because it was given much more attention than any other line. During each run we frequently returned to the m = 1/2 field for standardization.

Utilizing the theoretical equation for E_H we multiplied the normalized enhancement of each hyperfine transition by the average magnetic field used in its measurement and by the linewidth observed in the low power ESR. Numbers obtained in this way are nearly proportional to T_{1e}. Other corrections which may be applied are small but important. The ρ correction factor was calculated using the formula in the theoretical section with the assumption that $\tau_c = 3 \times 10^{-11}$ sec. The observed enhancements should be multiplied by this correction.

Our experimental apparatus, involving the flow system, makes enhancement a function of the total value of T_1(nuclear). If T_1(nuclear) is increased, enhancement does not build up to as large a value during the time the sample spends inside the microwave cavity. If T_1(nuclear) is decreased, enhancement decays more rapidly and falls to a lower value before reaching the NMR detection coil. These effects would require a magnetic field correction for an arbitrary concentration of VO^{2+} ions, but we choose a concentration at which the correction is small. In .01M VO^{2+} and at the flow rate used T_1(nuclear) is such that the observed enhancements are nearly independent of any small changes in T_1(nuclear) caused by changing the magnetic field. Beyond the limits of .005M and .02M enhancement becomes a strong function of T_1(nuclear).

Approximate σ corrections were calculated from the terms in Tables III and IV of reference 1 such as $S^{\pm}I_z$, $S^{\pm}I^{\pm}$ and $S^{\pm}I^{\mp}$. Included in $S^{\pm}I_z$ is a contribution due to other mechanisms α', which is the measured difference between Kivelson's theory and experiment. We make the reasonable assumption that $\alpha_1' = \alpha_2'$. It can be seen from Table IV that these σ corrections are no larger than our estimated experimental error in relative E_{100} of ± 19%.

Data are treated by multiplying all normalized, overlap corrected E_{100} values by the appropriate linewidths, including the small differences between $VOSO_4$ and $VO(ClO_4)_2$, and then applying other corrections to give a number proportional to $1/T_{1e}$. The equivalent of the 0.34 gauss excess linewidth of sulfate, assumed to be a T_{1e} contribution, is added to the $VO(ClO_4)_2$ data to make it comparable with $VOSO_4$. Numbers were then renormalized and averaged together. The result is a set of eight numbers which are proportional to $1/T_{1e}$, although the constant of proportionality is not known. These numbers are given at the bottom of Table IV.

The $1/T_{1e}$ data can be fit to a power series in m as shown in Table V. It is probably a good assumption that α_1 is equal to the α_1 predicted by Kivelson's theory plus the α_2' found from the linewidth data. If this assumption is made, one finds as shown in Table VI that γ_1 and δ_1 are in good agreement with theory as were γ_2 and δ_2, but β_1 like β_2 is smaller than predicted. Both β_1 and β_2 are about one gauss smaller than the numbers calculated from theory. This suggests that the theory is an error of about one gauss in the nonsecular contributions to β.

CONCLUSIONS

The results in Table VI show that the dynamic nuclear polarization spectrometer can yield precise relative T_{1e} values after proper treatment of the experimental data. The only appreciable deviations between the theory of relaxation[1] and our experimental data for VO^{+2} are in the terms linear in the nuclear magnetic quantum number. We also find that the term α_2' which is not explained in Kivelson's theory has a small field dependence in going from 1,000 to 3,000 gauss.

For other transition metal ions in aqueous solution VO^{+2} can be used as a reference in the dynamic nuclear polarization spectrometer, and it should be possible to measure absolute T_{1e} values for a variety of transition metal complexes.

ACKNOWLEDGEMENT- This work was performed under the auspices of the United States Atomic Energy Commission.

Table I

The Magnetic Parameters[a] for $VO(H_2O)_5^{+2}$

$g_\perp$	=	1.9778	$g_\parallel$	=	1.9312
g	=	$1/3\ (g_\parallel + 2g_\perp)$	=	1.9623	
Δg	=	$g_\parallel - g_\perp$	=	-0.0466	
$\frac{A_\perp}{g\beta}$	=	76.5 gauss	$\frac{A_\parallel}{g\beta}$	=	205.4 gauss
$\frac{a}{g\beta}$	=	$\frac{1}{3g\beta}\ (A_\parallel + 2\ A_\perp)$	=	119.5 gauss	
$\frac{b}{g\beta}$	=	$\frac{2}{3g\beta}\ (A_\parallel - A_\perp)$	=	86.0 gauss	

[a] Derived from a "glass" spectrum in 5.26M $HClO_4$ at 100°K.

Table II

Experimental and Calculated Linewidths of .01M $VOSO_4$ at 30°C

m	S-band Expt.[a]	Cal.[b]	X-band Expt.[c]	Cal.[d]
- 7/2	25.67	25.67	15.81	15.82
- 5/2	22.45	22.54	12.92	12.92
- 3/2	21.16	21.20	11.71	11.67
- 1/2	21.39	21.37	12.01	12.00
+ 1/2	22.77	22.68	13.78	13.78
+ 3/2	24.93	24.84	16.86	16.91
+ 5/2	27.44	27.49	21.24	21.32
+ 7/2	30.34	30.32	27.00	26.90

[a] At 3120 mc., 30.5° ± .5°C. units are gauss from first derivative peak to peak.

[b] Using $\alpha_2 = 21.90$, $\beta_2 = 1.333$, $\gamma_2 = .4977$, $\delta_2 = -.0544$.

[c] At 9070 mc., 30.0° ± 1°C.

[d] Using $\alpha_2 = 12.72$, $\beta_2 = 1.78$, $\gamma_2 = .705$, $\delta_2 = -.0157$.

Table III

Experimental and Theoretical[a] Linewidth Parameters For .01M $VOSO_4$ At 30°C.

Parameter	Expt.	Theoretical $\tau_c = 3.5 \times 10^{-11}$ sec.	Theoretical $\tau_c = 3.0 \times 10^{-11}$ sec.	Theoretical $\tau_c = 2.5 \times 10^{-11}$ sec.
X-band[c]				
α_2	12.72[b]	9.59	8.87	8.13
β_2	1.78	2.51	2.16	1.80
γ_2	.705	.685	.581	.476
δ_2	- .0157	- .0184	- .0158	- .0131
S-band[d]				
α_2	21.90[b]	16.01	14.43	12.64
β_2	1.333	2.84	2.33	1.95
γ_2	.4977	.604	.512	.422
δ_2	- .0544	- .0535	- .0459	- .0393

[a] Calculated from data in Table I of this paper and from coefficients in Tables III and IV of reference 1, assuming the correlation times listed.

[b] Measured values of α include other contributions α'.

[c] 9070 mc., 30 ± 1°C.

[d] 3120 mc., 30.5 ± .5°C.

Table IV

Enhancement Data and Correction Factors For .01M VO^{+2} at 30°C.

m	-7/2	-5/2	-3/2	-1/2	1/2	3/2	5/2	7/2
Sulfate E_{100}[a]	1.4605(2)	1.4883(2)	1.3471(2)	1.1892(3)	1.0000(2)	.8127(4)	.6728(2)	.5689(2)
Overlap	.1222	.2060	.1599	.1231	.0917	.0663	.0534	.0326
Perchlorate E_{100}	1.4087(1)	1.5457(3)	1.4179(3)	1.2486(3)	1.0000(5)	.9194(3)	.7397(4)	.6147(3)
Overlap	.1286	.2020	.1664	.1276	.0989	.0755	.0620	.0355
Ho[b]	697.4	777.5	868.6	971.5	1086.8	1217.7	1359.3	1512.3
ρ Term[c]	8.944	8.825	8.648	8.422	8.149	7.846	7.528	7.214
σ Term[d]	.9987	.9959	1.0039	.9980	.9980	1.0013	1.0072	1.0058
$1/T_{1e}$[e]	.8610	.8951	.9415	.9514	1.0000	.9747	.9943	.9853

[a] Numbers in parentheses are the number of runs this line was observed. After partial analysis sulfate and perchlorate data are averaged, weighted according to the number of observations.

[b] Approximate line center fields.

[c] ρ term = $1/8 \sum_m (3 + 7/1 + \omega^2 \tau_c^2)$.

[d] σ term described in text.

[e] Renormalized to m = 1/2.

Table V

Comparison of Experimental and

Calculated Relative Spin Lattice Relaxation Times

m	$1/T_1$ Expt.	$1/T_1$ Calc.[a]	Expt.-Calc.
-7/2	.8610	.8590	.0020
-5/2	.8951	.8967	-.0016
-3/2	.9415	.9293	.0122
-1/2	.9514	.9560	-.0046
1/2	1.0000	.9760	.0240
3/2	.9747	.9883	-.0136
5/2	.9943	.9921	.0021
7/2	.9853	.9866	-.0013

[a] Calculated from $\alpha_1 = .9669$, $\beta_1 = .200$, $\gamma_1 = -.0035$ and $\delta_1 = -.000145$ which convert in gauss units assuming $\alpha_1' = \alpha_2'$ as $\alpha_1 = (16.68)$, $\beta_1 = .345$, $\gamma_1 = -.062$ and $\delta_1 = -.022$.

Table VI

Comparison of Experimental and Theoretical $1/T_1$ Parameters

Term	Theoretical[a]	Experimental[b]
α_1	16.68[c]	(16.68)[d]
β_1	1.28	.35
γ_1	- .062	- .062
δ_1	- .023	- .025

[a] From nonsecular terms only in Tables III and IV of Reference 1. Assuming $\tau_c = 3 \times 10^{-11}$ sec. and using data from Table I, this paper.

[b] Assuming $\tau_c = 3 \times 10^{-11}$ sec.

[c] Includes 7.47 gauss α_1' correction assuming $\alpha_1' = \alpha_2'$. This and all other numbers in this table given in units of gauss contribution to total linewidth.

[d] Assumed, in order to establish a scale for evaluation of the other parameters.

REFERENCES

1. R. Wilson and O. Kivelson, J. Chem. Phys. 44, 154(1966).
2. Singer and Johnson, Rev. Sci. I. 30, 92(1959).
3. R. G. Hayes and R. J. Myers, J. Chem. Phys. 40, 877(1964).
4. (a) A. Abragam, Phys. Rev. 98, 1729(1955); (b) A. Abragam, "The Principles of Nuclear Magnetism," Oxford Univ. Press, London (1961), Chapter VIII.
5. Rodgers and Pake, J. Chem. Phys. 33, 1107(1960).
6. D. Kivelson, J. Chem. Phys. 33, 1094(1960).
7. B. Spencer, "Electron Spin Resonance Studies of Transition Metal Ion Complexes," UCRL-16175 (Ph.D. Thesis).
8. P. W. Atkins and D. Kivelson, J. Chem. Phys. 44, 169(1966).
9. Unpublished experiments by Dr. Kurt Wüthrich in H_2O and D_2O from 20-160°C.

Figure Captions

Figure 1. Block diagram of dynamic nuclear polarization spectrometer.

Figure 2. Parabolic S-band cavity used in DNP spectrometer. The arrows show the direction of sample flow.

Figure 3. Quartz S-band cavity used in ESR spectrometer. The outside of the cavity is silvered and it is attached at the upper end to S-band wave guide.

Figure 4.(a) ESR spectrum of 0.01 M $VOSO_4$ at 9070 mc and 30°C.

(b) ESR spectrum of 0.01 M $VOSO_4$ at 3120 mc and 30°C.

Figure 5. The enhancement spectrum in the region of the m = 1/2 transition of VO^{+2}. The points are experimental and the curve uses Lorentzian line shape functions with line widths derived from the ESR spectrum.

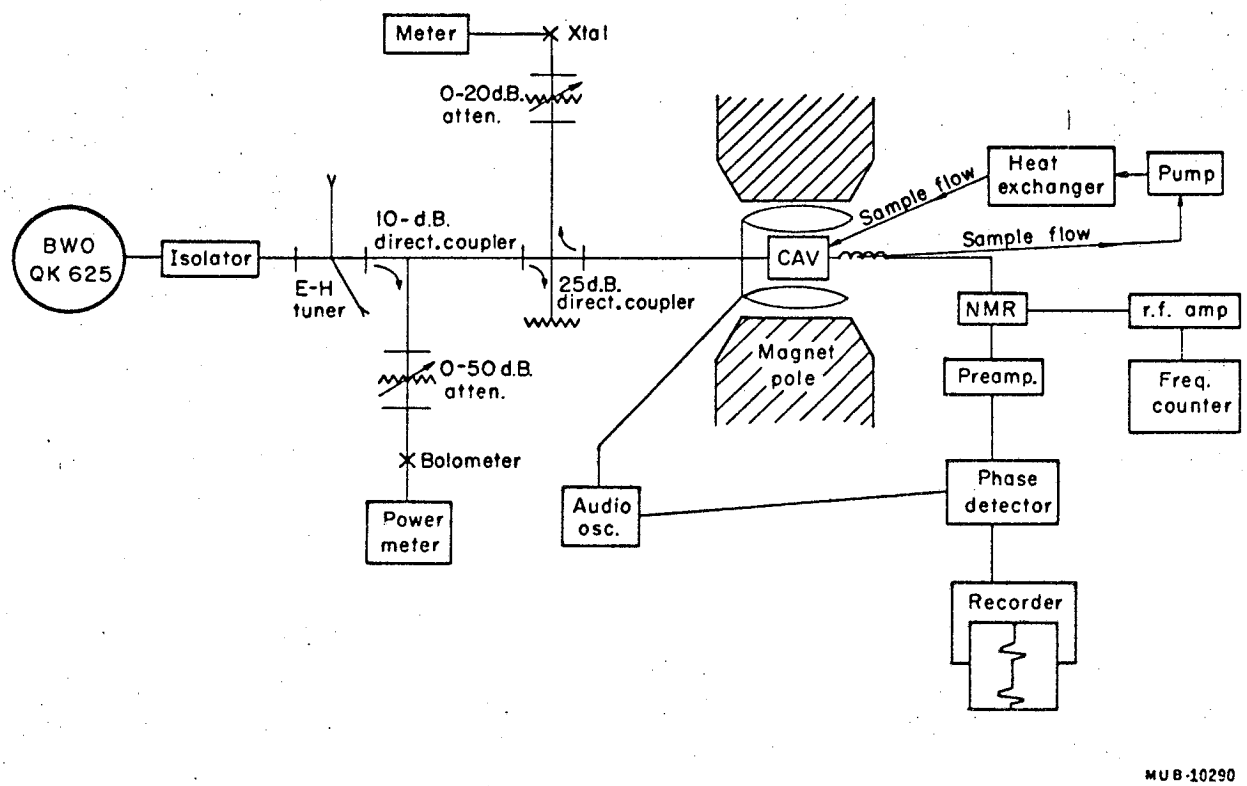
Meter
Xtal
0-20d.B.
atten.
BWO
QK 625
Isolator
E-H
tuner
10-d.B.
direct.coupler
25d.B.
direct.coupler
0-50 d.B.
atten.
Bolometer
Power
meter
Audio
osc.
Magnet
pole
CAV
Sample flow
Sample flow
Heat
exchanger
Pump
NMR
r.f. amp
Preamp.
Freq.
counter
Phase
detector
Recorder
MUB-10290

Fig. 1

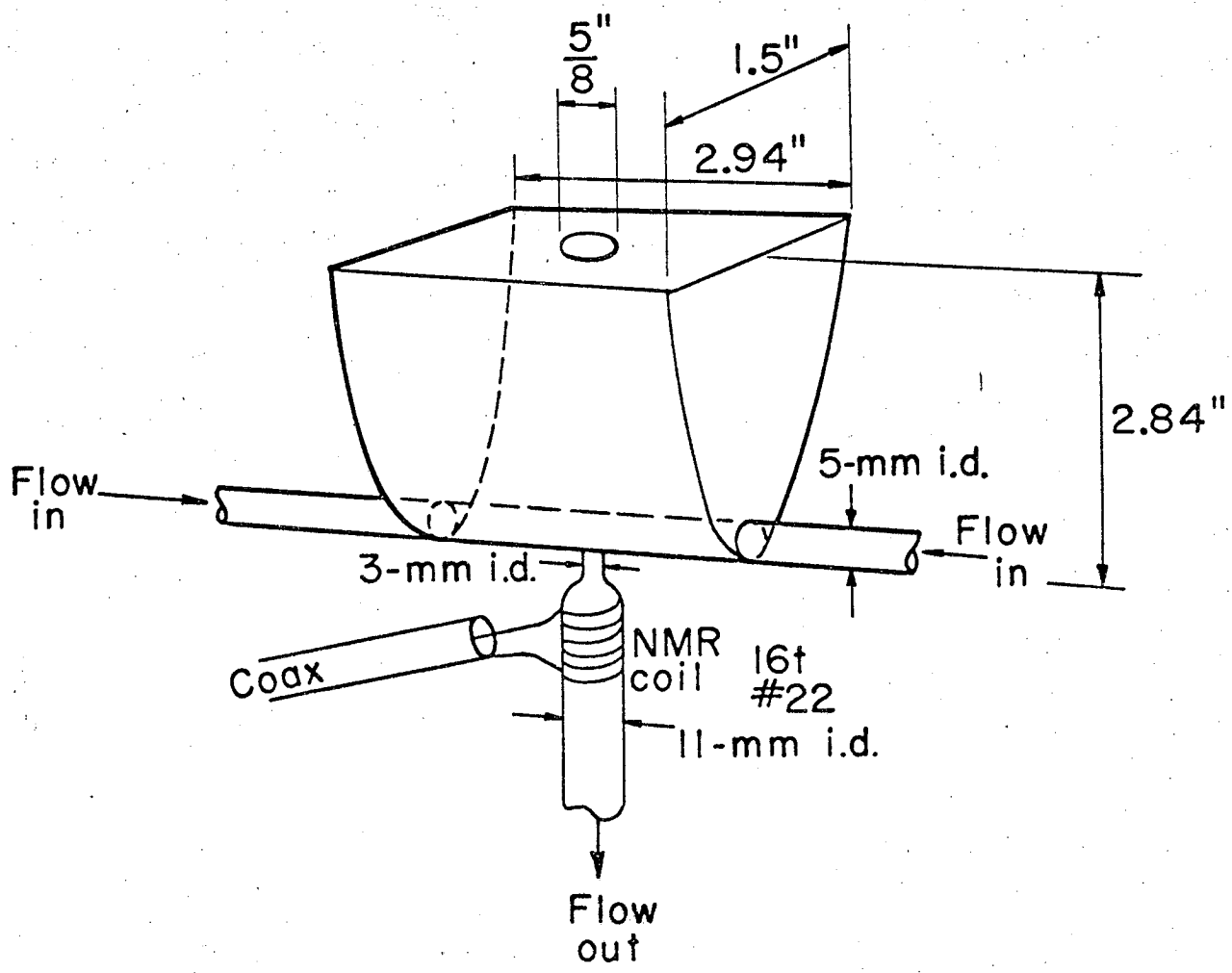

MUB-10291

Fig. 2

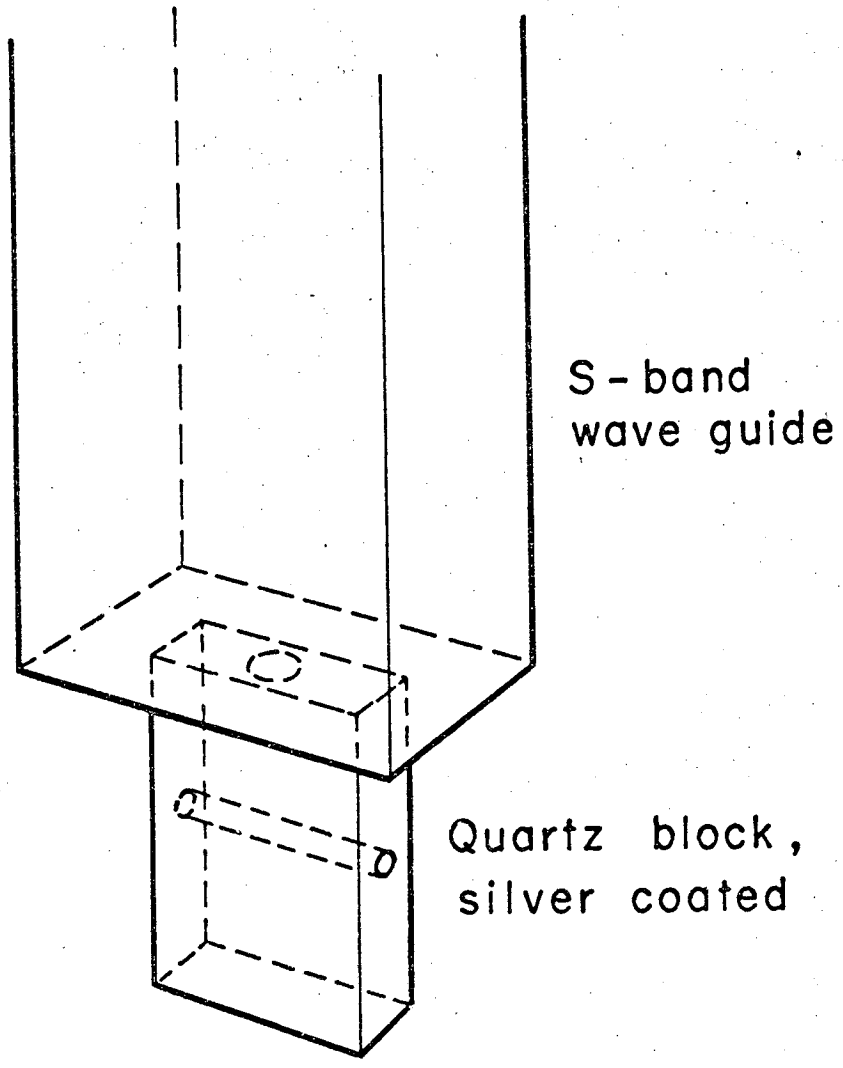

Fig. 3

MUB-10292

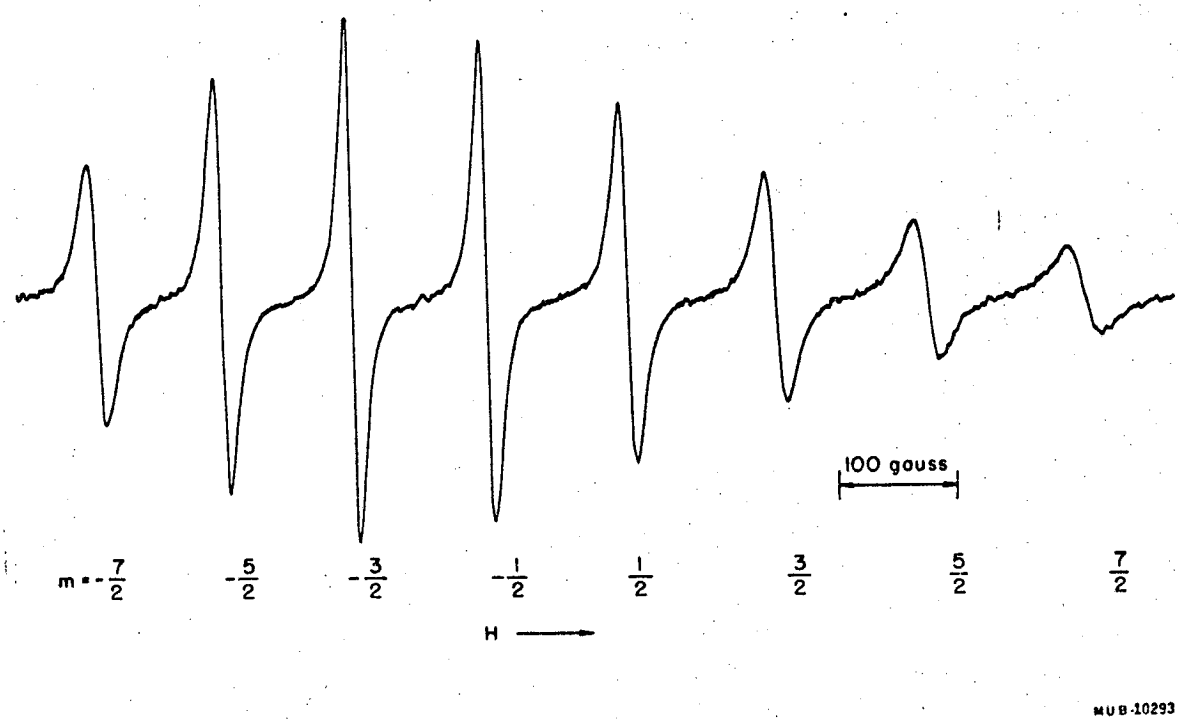

Fig. 4

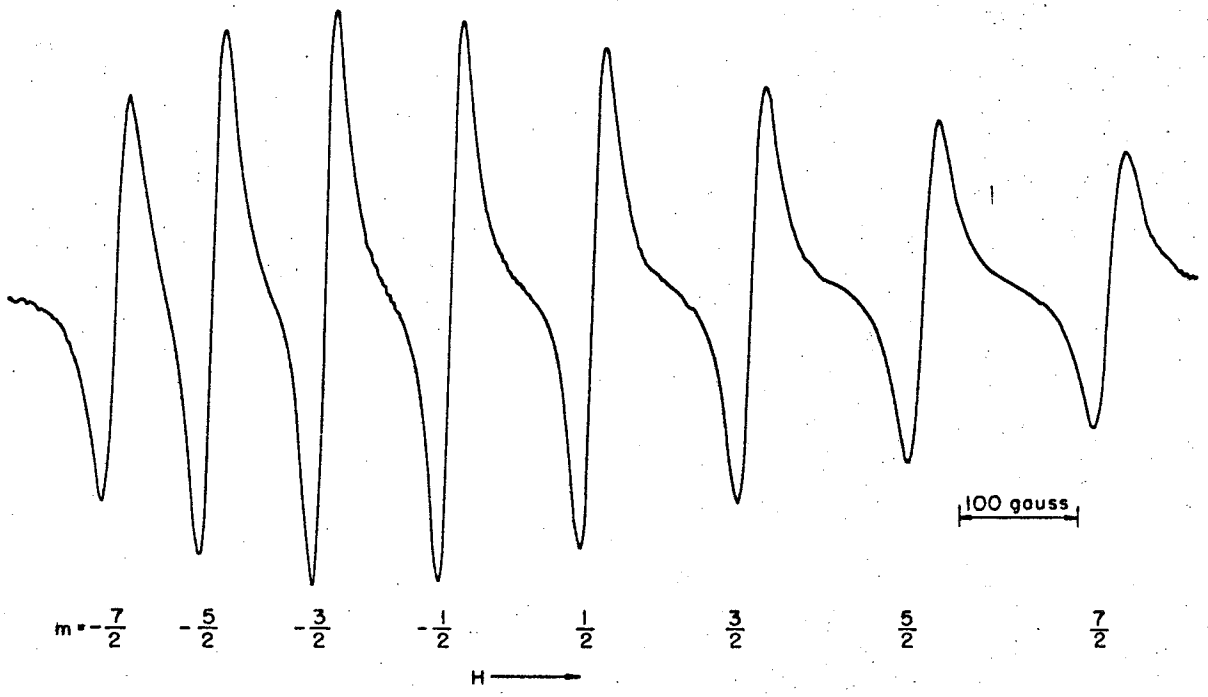

MUB-10294

Fig. 4b

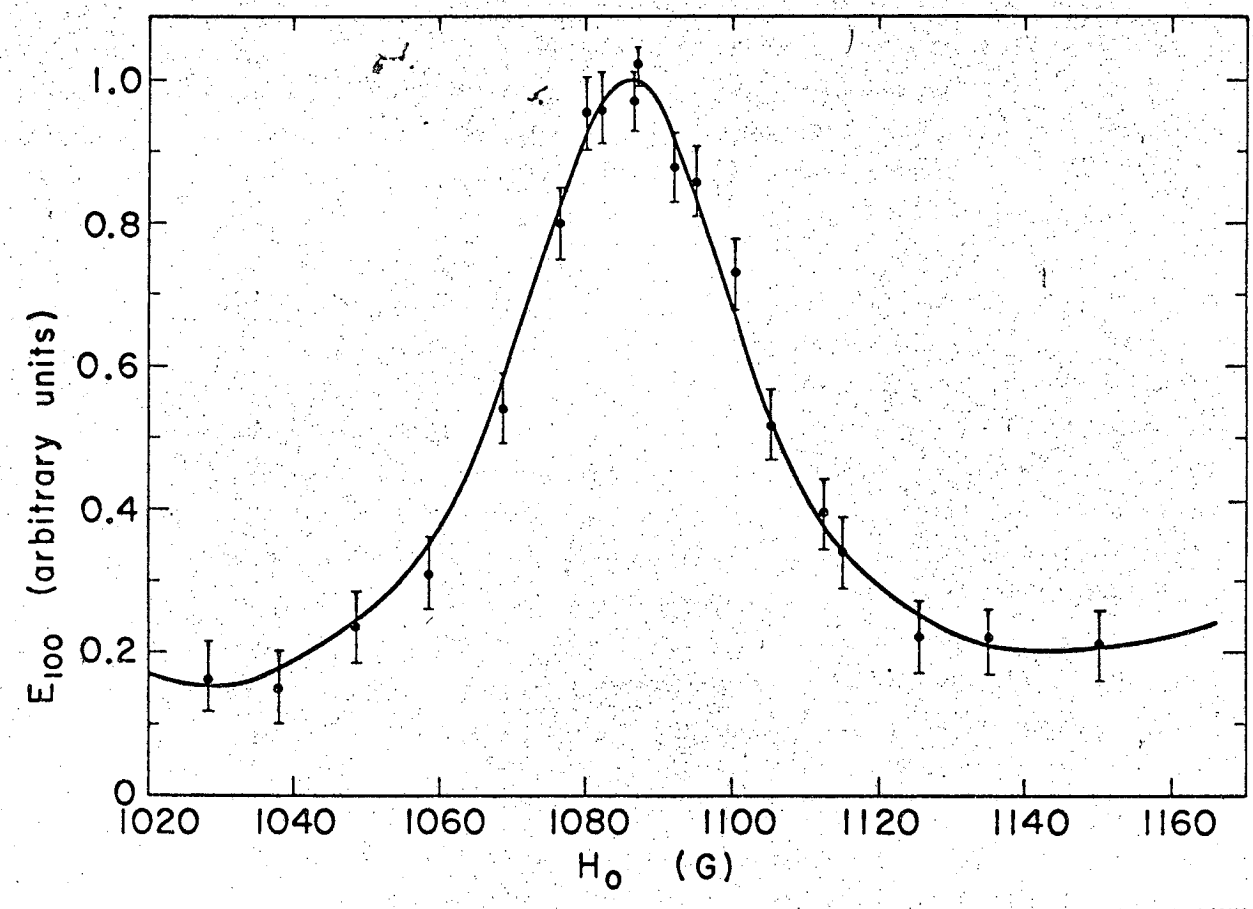

MUB-10426

Fig. 5

This report was prepared as an account of Government sponsored work. Neither the United States, nor the Commission, nor any person acting on behalf of the Commission:

A. Makes any warranty or representation, expressed or implied, with respect to the accuracy, completeness, or usefulness of the information contained in this report, or that the use of any information, apparatus, method, or process disclosed in this report may not infringe privately owned rights; or

B. Assumes any liabilities with respect to the use of, or for damages resulting from the use of any information, apparatus, method, or process disclosed in this report.

As used in the above, "person acting on behalf of the Commission" includes any employee or contractor of the Commission, or employee of such contractor, to the extent that such employee or contractor of the Commission, or employee of such contractor prepares, disseminates, or provides access to, any information pursuant to his employment or contract with the Commission, or his employment with such contractor.